PERGAMON

Polyhedron 18 (1999) 1189–1200

POLYHEDRON

Synthesis and characterization of ruthenium, rhenium and titanium formate, acetate and trifluoroacetate complexes. Correlation of IR spectral properties and bonding types

Dorothy H. Gibson*, Yan Ding, Rebecca L. Miller, Bradley A. Sleadd, Mark S. Mashuta, John F. Richardson

Department of Chemistry and Center for Chemical Catalysis, University of Louisville, Louisville, KY 40292, USA

Received 10 July 1998; accepted 12 October 1998

Abstract

New formate (**1**–**3**; **4b**, **6** and **7**), acetate (**8**, **9**) and trifluoroacetate (**12**, **13** and **15**) complexes have been synthesized and characterized by elemental analysis and by IR and ^{1}H and ^{13}C NMR spectroscopies. New data or new synthetic procedures are provided for several known complexes (**4a**, **5**, **19**, **11** and **14**). X-ray structural data for *cis*-$Ru(bpy)_2(CO)(OCHO)(PO_2F_2)$ (**4b**) clearly identify the η^1-bound formate ligand bound to an octahedral ruthenium center and the data for *fac*-$Re(CO)_3(PPh_3(OCOMe)$ (**9**) show an η^2-bound acetate ligand bound to an octahedral rhenium center. Infrared spectral data for four types of formate complexes, three bonding types of acetates and the two known types of trifluoroacetate ligands are discussed. Comparisons of the ν_{OCO} bands for the carboxylate ligands in all of the complexes show that these bands are useful in identifying the bonding type of each carboxylate ligand.

Keywords: Infrared spectra; Crystal structures; Spectra/structure correlations; Synthetic methods

Interest in the catalytic hydrogenation of CO_2 to formate or formic acid by metal complexes as well as in the decomposition of formic acid on metal surfaces has resulted in increased interest in metal complexes with formate ligands [1–6]. In particular, the vibrational spectral bands of the carboxylate groups in such model compounds can be of assistance in the characterization of surface-bound formate [7–10]. However, the utility of this approach has been somewhat limited in the past by the lack of structurally characterized compounds for which both ν_{OCO} bands have been reported. In particular, the lower-frequency ν_{sym} band has frequently not been identified in compounds which were structurally characterized. Efforts to correlate carboxylate IR spectral bands with structural types have been made earlier [11–13]; thus, the general region where the bands will be found is well known. However, the previous work was done without the benefit of as much structural data to support the assignments of bonding types as is available now. Furthermore, a few new bonding types have been identified since the earlier efforts to correlate spectra and structural data.

We describe herein the synthesis and characterization of several new formate, acetate and trifluoroacetate complexes and discuss the relationships between their bonding types and IR spectral characteristics together with the structural characterizations of two of the new compounds. With all of the compounds which we have prepared, the IR spectral data have been obtained by solid-state techniques (see Section 3) in order to compare the IR data with X-ray structural data wherever possible. Also, representative spectra are provided for a number of compounds which illustrate intensity differences in the carboxylate bands for differing structural types.

1. Results and discussion

1.1. Synthesis of new compounds

New formate complexes prepared for the present study are of three types: η^1 (bound to the metal by a single carboxylate oxygen), η^2 (bound to a single metal through

*Corresponding author. Tel.: +1-502-8525977; fax: +1-502-8525977; e-mail: dhgibs01@athena.louisville.edu

0277-5387/99/$ – see front matter
PII: S0277-5387(98)00414-8

both carboxylate oxygens) and μ_2–η^2 (bound through both carboxylate oxygens to two different metal centers). In all cases, the η^1-type complexes have been used as precursors to the other two types.

We prepared the η^1-coordinated formates by reactions of the corresponding methyl or hydrido complexes with formic acid; the compounds are *cis*-$Re(CO)_4(PPh_3)(\eta^1$-OCHO) (**1**), $Cp_2Ti(CH_3)(\eta^1$OCHO) (**2**) and $CP_2Ti(\eta^1$-$OCHO)_2$ (**3**) and *cis*-$Ru(bpy)_2(CO)(\eta^1$-$OCHO)^+PF_6^-$ (**4a**; bpy=2,2′-bipyridyl). Compound **4a** has been reported previously [14], but full characterization data was not provided. The PO_2F_2 salt of the same cation (**4b**) is new and was formed as the result of hydrolysis of the PF_6 salt during synthesis (as observed previously with this anion [15]); structural data for **4b** are discussed below. The new compounds have also been characterized by elemental analysis and spectral data. We reported structural data for **3** previously [16]; spectral and analytical data for it are provided in Section 3. Also, a new synthesis of the known [17,18] compound, *mer, trans*-$Re(CO)_3(PPh_3)_2(\eta^1$-OCHO) (**5**), was accomplished by treating the corresponding hydride complex with formic acid; the spectral properties of the product were identical to those reported previously.

The known [18] η^2-coordinated formate, *cis, trans*-$Re(CO)_2(PPh_3)_2(\eta^2$-OCHO) (**6**), was prepared for the present study by thermolysis of the corresponding η^1-complex, **5**. The product had IR spectral properties which were identical to those reported earlier.

As noted previously [11–13], carboxylate anions bridged between two identical metal centers, and via both oxygen atoms in μ_2–η^2 fashion, can assume any of the geometries shown in Fig. 1 for formate ion unless the metal atoms are bound together or connected by other bridging ligands; in the latter cases, only the syn, syn isomers are possible. Also, if the metal centers are different, two isomers of the anti, syn type are possible. The structurally characterized formate complexes of the μ_2–η^2 type which are discussed below are all metallacycles where the formate is constrained to be in the syn, syn mode; several have more than one such formate bridge [19]. The new complex, *cis, cis*-$Re(CO)_4(PPh_3)(\mu_2$-η^2-$OCHO)^+BF_4^-$ (**7**), was prepared by reaction between the monodentate complex **1** and *cis*-$Re(CO)_4(PPh_3)(F$-$BF_3)$ [20]; it has been characterized by elemental analysis and spectral data. The geometry about the formate ion in **7** is not known and, in fact, samples of **7** may contain a mixture of isomers.

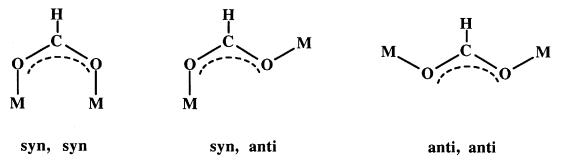

Fig. 1. Coordination geometries for μ_2–η^2–type formate complexes.

The new monodentate acetate complex, *cis*-$Ru(bpy)_2(CO)(\eta^1$-$OCOCH_3)$ (**8**), was prepared by heating the corresponding hydride complex with acetic acid. The product was characterized by elemental analysis and spectral data.

The bidentate acetate complex, *fac*-$Re(Co)_3(PPh_3)$ (η^2-$OCOCH_3$) (**9**), was obtained after prolonged heating of *cis*-$Re(CO)_4(PPh_3)(CH_3)$ with acetic acid. The compound was characterized by elemental analysis, spectral data and by X-ray crystallography (see below) which established the facial geometry of the carbonyl ligands and the η^2 nature of the acetate ligand with certainty.

An alternate method was used for the preparation of the known [17] complex, *cis, trans*-$Re(CO)_2(PPh_3)_2$-(η^2-$OCOCH_3$) (**10**); in our procedure, *mer, trans*-Re-$(CO)_3(PPh_3)_2(H)$ [21] was heated with acetic acid for several hours to obtain the bidentate acetate complex. The compound was obtained in high yield and had spectral properties which were in agreement with those reported previously.

A sample of *fac*-$Mn(CO)_3(PPh_3)(\eta^2$-$OCOCH_3)$ (**11**) was available from previous work [22]. The assignment of facial geometry was made on the basis of characteristic IR spectral bands for the terminal carbonyls in the compound which are closely related to those of the analogous rhenium complex, **9**, that has been fully characterized.

The new trifluoroacetate complexes, $Cp_2Ti(CH_3)(\eta^1$-$OCOCF_3)$ (**12**) and *cis*-$Re(CO)_4(PPh_3)(\eta^1$-$OCOCF_3)$ (**13**) were made by treating the corresponding methyl complexes with trifluoroacetic acid. Samples of the known [17,23] *mer, trans*-$Re(CO)_3(PPh_3)_2(\eta^1$-$OCOCF_3)$ (**14**) and the new *cis*-$[Ru(bpy)_2(CO)(\eta^1$-$OCOCF_3)]PF_6$ (**15**), were obtained by treating the corresponding hydride complexes with the acid. The greater acidity of CF_3COOH allows much milder conditions to be used in this procedure than with the preparations of formate and acetate complexes. The new compounds were characterized by elemental analysis and spectral data.

1.2. Structural characterizations

The solid state structures of **4b** and **9** have been established by X-ray crystallography. The ORTEP diagram for **4b** is shown in Fig. 2; the diagram for **9** is shown in Fig. 3. The crystal data for both compounds are summarized in Table 1. Selected bond distances and bond angles are shown in Table 2. The formate ligand is clearly monodentate, with unequal O–C bond lengths of 1.151(7) Å and 1.224(8) Å and a carboxyl O–C–O angle of 127.0(7) Å; the coordination geometry about the ruthenium atom is distorted octahedral. The Ru–N bond that is trans to the terminal carbonyl ligand is longer, at 2.112(5) Å than the Ru–N bonds which are cis to this ligand (both approximately 2.06 Å) as is commonly seen for cations of the general type *cis*-$Ru(bpy)_2(CO)(X)^+$

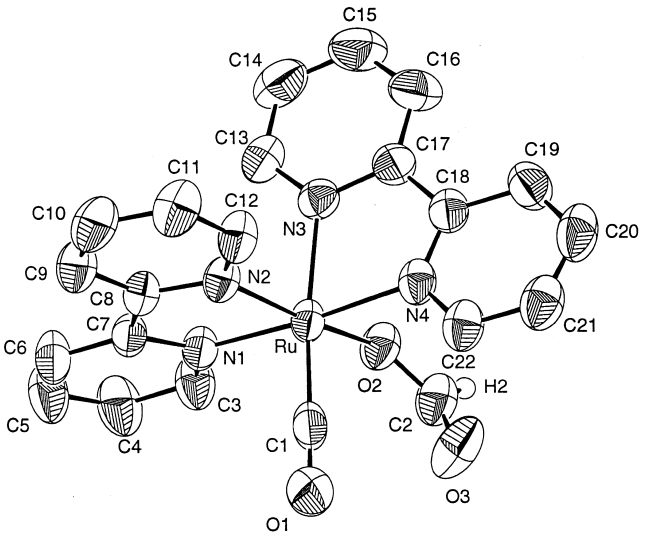

Fig. 2. ORTEP drawing of **4b** (cation only) with thermal ellipsoids shown at the 50% probability level.

[24–27]. Selected bond distances and bond angles are shown in Table 3. The geometry about the rhenium atom in **9** is also best described as distorted octahedral. The bidentate carboxyl O–C–O angle is 121.2(4)° and is substantially larger (112.7(7)°) than in the complex having a chelated CO_2 ligand, from a metallocarboxylate moiety, bound through both oxygen atoms to this metal fragment as the result of μ_2–η^3 bridging [28]. The Re–C bond length for the carbonyl ligand trans to triphenylphosphine in **9** is slightly longer, at 1.957(4) Å, than for those cis to this ligand (1.889(4) and 1.892(4) Å). The O–Re bond lengths are similar in length (2.182(2) and 2.210(3) Å),

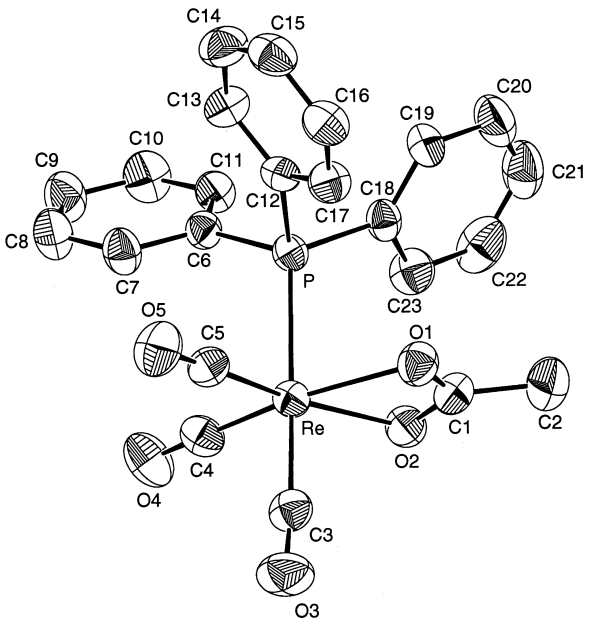

Fig. 3. ORTEP drawing of **9** with thermal ellipsoids shown at the 50% probability level.

giving rise to a symmetrically chelated acetate ligand. The structure is closely similar to that for *cis, trans*-Re-$(CO)_2(PPh_3)_2(\eta^2$-$OCOCH_3)$ reported by La Monica, et al. [18].

Crystallographic data for $Cp_2Ti(OCHO)_2$ with two monodentate formate ligands, have been reported by us previously [16]. The O–C–O bond angles, 126.7(3)° and 127.2(3)°, are slightly larger than for the ruthenium complex **4b**; however, the carboxylate O–C bond lengths are similar to those of **4b** at 1.188(4) Å and 1.275(4) Å.

1.3. IR spectral data

The region from 1800 to 950 cm^{-1} of the DRIFTS (see Section 3) spectra for the η^1-type formate complexes **1** and **5** are shown in Fig. 4 together with that of the μ_2–η^2-coordinated formate **7**; spectral data for another η^1 complex, **4a**, is shown in Fig. 5. All of the complexes in Fig. 4 contain triphenylphosphine ligands and thus show the characteristic pair of weak bands at approximately 1430 and 1480 cm^{-1}; typically, the lower frequency band is more intense. Compounds with this phosphine ligand also show a low frequency band, of similar intensity, at approximately 1100 cm^{-1}. The ν_{OCO} bands for the formate ligand in each of these complexes (see Table 4 for assignments) are weak to medium in intensity, but are clearly more intense than the pair of bands for the phosphine ligand in the 1450 cm^{-1} region in each compound. The ν_{sym} band in the μ_2–η^2-type complex **7** is broad and has several shoulders on it as does the weaker ν_{asym} band. These features were reproduced for several different samples of the compound; since spectral data for other complexes of this type have not been reproduced, it is unclear whether this pattern is characteristic of compounds with bridging formate ligands of this type or whether it is due to the presence of multiple geometric forms of the bridging formate ligands (as discussed above) in the sample. Partial spectra for an η^2 complex, **6**, are shown in Fig. 6. Note that the carboxylate bands have both moved relative to those of the η^1 complexes: the ν_{asym} band is now at 1547 cm^{-1} and the ν_{sym} band is at 1358 cm^{-1} also, both bands are greatly diminished in intensity as compared with the corresponding bands in the η^1 complex.

The ν_{OCO} bands for formate complexes in four distinct bonding modes are collected in Table 4 and include data from our new complexes as well as data from well-chararacterized compounds prepared by other groups previously. In addition to the three general types described above, one recently characterized compound has a single carboxylate oxygen bridged between two titanium centers, providing a μ_2–η^1 bridging formate ligand [29]. Although not the first structural report of a compound with this bonding mode [30–33], it is the first for which the carboxylate bands in IR spectral data can be readily identified.

Table 1
Summary of crystallographic data for $[Ru(bpy)_2(CO)(OCHO)]PF_2O_2$ (**4b**) and $Re(CO)_3(PPh_3)(OCOCH_3)$ (**9**)

	4b	**9**
Formula	$C_{22}H_{17}F_2N_4O_5PRu$	$C_{23}H_{18}O_5PRe$
Formula weight	587.44	591.57
Cryst dimens, mm	0.43×0.25×0.17	0.40×0.36×0.33
Cryst descripn	yellow block	colorless block
Crystal system	triclinic	monoclinic
Space group	$P\bar{1}$	$P2_1/n$
a, Å	11.018 (3)	13.229 (3)
b, Å	13.819 (3)	10.523 (2)
c, Å	7.949 (3)	15.683 (2)
α, deg	99.79 (2)	
β, deg	98.90 (2)	93.69 (1)
γ, deg	76.25 (2)	
Vol. Å^3	1150.2 (6)	2178.7 (6)
Z	2	4
D_c, g cm^{-3}	1.696	1.803
μ(Mo K$_\alpha$) cm^{-1}	8.10	56.84
Diffractometer	Enraf-Nonius CAD4	Enraf-Nonius CAD4
Monochromator	graphite crystal	graphite crystal
Radiation (λ, Å)	MoK$_a$ (λ=0.71073)	MoK$_a$ (λ=0.71073)
Temp, °C	23 (1)	23 (1)
Scan range, deg	0.85+0.35 tan θ	0.75+0.35 tan θ
Scan speed, deg/min	1–5	1–5
Maximum 2θ, deg	50.0	55.0
Abs. corr.	PSI Scans	PSI Scans
Transmission factors: min/max	0.9110/1.0000	0.8592/1.0000
No. unique reflns collected	4042	53/2
No. reflns included ($I_0>3\sigma$ (I_0))	3266	3808
No. of params	344	272
Computer hardware	Silicon Graphics	Silicon Graphics
Computer software	teXsan (msc)	teXsan (msc)
Residuals: *R*; R_w	0.055; 0.055	0.022; 0.022
GOF	3.27	1.38
Least squares weights	$[\sigma^2(F_0)]^{-1}$	$[\sigma^2(F_0)]^{-1}$
Maximum peak in final diff. map	1.71 e$^-$/Å^3	0.65 e$^-$/Å^3
Minimum peak in final diff. map	−1.03 e$^-$/Å^3	−0.60 e$^-$/Å^3

[a] $R=\Sigma\ \||F_0|-|F_c|\|/\Sigma\ |F_0|$; $R_w=[\Sigma\ w(|F_0|-|F_c|)^2]/\Sigma\ wF_0^2]^{1/2}$.

Table 2
Selected bond distances (Å) and Angles (°) for $[Ru(bpy)_2(CO)(OCHO)]PF_2O_2$ (**4b**)

Bond distances			
Ru–O(2)	2.060(4)	Ru–N(1)	2.057(5)
Ru–N(2)	2.061(5)	Ru–N(3)	2.112(5)
Ru–N(4)	2.072(5)	Ru–C(1)	1.838(8)
O(1)–C(1)	1.151(7)	O(2)–C(2)	1.253(8)
O(3)–C(2)	1.224(8)		
Bond angles			
O(2)–Ru–N(1)	93.5(2)	O(2)–Ru–N(2)	167.4(2)
O(2)–Ru–N(3)	81.9(2)	O(2)–Ru–N(4)	85.6(2)
O(2)–Ru–C(1)	96.2(2)	N(1)–Ru–N(2)	78.5(2)
N(1)–Ru–N(3)	96.7(2)	N(1)–Ru–N(4)	174.7(2)
N(1)–Ru–C(1)	89.4(2)	N(2)–Ru–N(3)	89.3(2)
N(2)–Ru–N(4)	101.5(2)	N(2)–Ru–C(1)	93.5(2)
N(3)–Ru–N(4)	78.1(2)	N(3)–Ru–C(1)	173.7(2)
N(4)–Ru–C(1)	95.8(2)	Ru–O(2)–C(2)	125.4(5)
Ru–C(1)–O(1)	178.8(6)	O(2)–C(2)–O(3)	127.0(7)

Table 3
Selected bond distances (Å) and angles (°) for $Re(CO)_3(PPh_3)(\eta^2$-$OCOCH_3)$ (**9**)

Bond distances			
Re–P	2.4951(9)	Re–O(1)	2.210(3)
Re–O(2)	2.182(2)	Re–C(3)	1.957(4)
Re–C(4)	1.889(4)	Re–C(5)	1.892(4)
O(1)–C(1)	1.280(5)	O(2)–C(1)	1.266(5)
O(3)–C(3)	1.123(4)	O(4)–C(4)	1.152(5)
O(5)–C(5)	1.148(4)	C(1)–C(2)	1.491(6)
Bond angles			
P–Re–O(1)	84.58(7)	P–Re–O(2)	89.88(7)
P–Re–C(3)	176.6(1)	P–Re–C(4)	93.9(1)
P–Re–C(5)	89.5(1)	O(1)–Re–O(2)	59.42(9)
O(1)–Re–C(3)	94.7(1)	O(1)–Re–C(4)	163.9(1)
O(1)–Re–C(5)	109.2(1)	O(2)–Re–C(3)	92.6(1)
O(2)–Re–C(4)	104.6(1)	O(2)–Re–C(5)	168.6(1)
C(3)–Re–C(4)	87.7(2)	C(3)–Re–C(5)	87.6(2)
C(4)–Re–C(5)	86.8(2)	Re–O(1)–C(1)	90.7(2)
Re–O(2)–C(1)	92.4(2)	O(1)–C1–O(2)	117.5(4)
O(1)–C(1)–C(2)	121.2(4)	O(2)–C(1)–C(2)	121.1(4)
Re–C(3)–O(3)	176.2(4)	Re–C(4)–O(4)	178.5(4)
Re–C(5)–O(5)	178.7(3)		

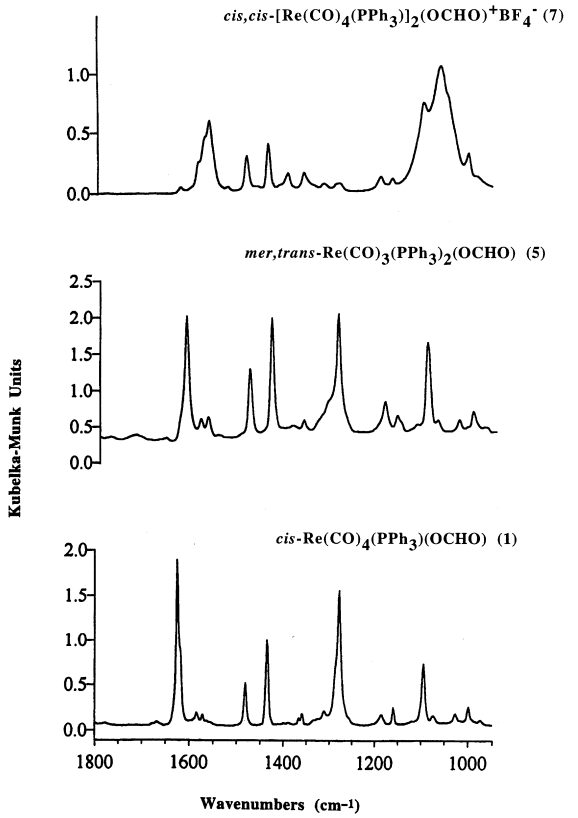

Fig. 4. DRIFTS spectra (1800–950 cm^{-1}) for complexes **1**, **5**, and **7**.

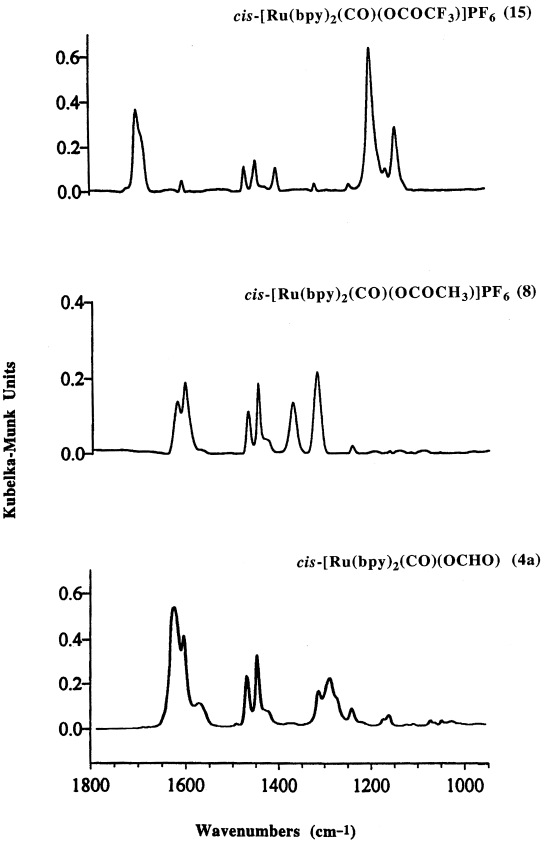

Fig. 5. DRIFTS spectra (1800–950 cm^{-1}) for complexes **4a**, **8**, and **15**.

In the example compounds, those with η^1-coordinated formate ligands show the carboxyl ν_{asym} band in the region 1603–1652 cm^{-1} and the ν_{sym} band at 1253–1329 cm^{-1}; the median value of $\Delta\nu$ is 337 cm^{-1}. In some cases, isotopic labeling has been done to provide further confirmation of carboxylate band assignments. For example, the IR spectrum of the structurally characterized *trans*-Ru(dmpe)$_2$(η^1-OCHO)(H) shows bands for the carboxylate at 1603 and 1329 cm^{-1}; use of $^{13}CO_2$ in the preparation of the compound gives a product with these bands lowered to 1564 and 1309 cm^{-1}, respectively [34]. This technique is certainly necessary when there is severe overlapping of bands from other ligands with those of the carboxylate group. Usually, however, it is not necessary now because the general position of these bands is well known [11–13] and comparisons with spectra from other closely related compounds in a series (e.g., those with a halide instead of a carboxylate ligand, but otherwise the same) will usually allow the identification of the ν_{OCO} bands to be done.

The η^2- and μ_2–η^2-types of chelated complexes, for which data is shown in Table 4, exhibit the ν_{asym} band well below 1600 cm^{-1} and the ν_{sym} band appears above 1300 cm^{-1}. The asymmetric stretching band in the compounds with bridging ligands appears at slightly higher frequency than the ν_{asym} band in compounds having both carboxyl oxygens bound to a single metal. This results in a median value of $\Delta\nu$ for the bridging type of 225 cm^{-1} while $\Delta\nu$ for the η^2-type is 216 cm^{-1} for the available examples; clearly, it is not a large enough difference to be definitive. Although the compounds in Table 4 vary from metallocenes with pseudotetrahedral geometry at the metal to square planar and octahedral complexes, there is not yet any discernible pattern of dependence of the band positions in these compounds on structural factors or geometry at the metal center.

The single example compound with a μ_2-η^1-coordinated formate ligand shows the carboxyl ν_{asym} band at 1664 cm^{-1}, well above the analogous band in simple η^1-type complexes. Also, the ν_{sym} band is at much lower frequency (1205 cm^{-1}) than in the η^1 complexes, leading to a large $\Delta\nu$ of 459 cm^{-1} which easily identifies the bonding type as distinct from the others.

Examination of the DRIFTS spectra in the region 1800–950 cm^{-1} for an η^1 acetate, as illustrated by **8** in Fig. 5, shows the problem which attends the assignment of bands for the carboxylate stretching vibrations in acetate complexes. There are three vibrations for the acetate ligand in this region: ν_{asym} and ν_{sym} for the carboxylate and δ_{C-H} for the methyl group. For **8**, the band at 1605 cm^{-1} and the series of weak bands centered at approximately 1470 cm^{-1} are due to the bipyridine ligand; the bands at 1621, 1380 and 1317 cm^{-1} are due to the acetate ligand. By analogy

Table 4
Carboxylate stretching frequencies of formate complexes

Compound	Structure assignment	Bonding	ν_{asym} (CO_2)	ν_{sym} (CO_2)	$\Delta\nu$	Ref
$Cp_2Ti(CH_3)(OCHO)$ (**2**)	spectroscopy	η^1	1652, 1636	1270, 1253	366–399	[a]
$Cp_2Ti(OCHO)_2$ (**3**)	X-ray	η^1	1644	1290 (1273)	354 (371)	[a], [15]
trans-$(PCy_3)_2Pt(H)(OCHO)$	X-ray	η^1	1620	1310	310	[41]
$CpFe(CO)_2(OCHO)$	X-ray	η^1	1620	1293	327	[3]
fac-Re(bpy)$(CO)_3(OCHO)$[b]	X-ray	η^1	1630	1280	350	[42,43]
cis-$Re(CO)_4(PPh_3)(OCHO)$ (**1**)	spectroscopy	η^1	1625	1278	347	[a]
mer, trans-$Re(CO)_3(PPh_3)_2(OCHO)$ (**5**)	spectroscopy	η^1	1616	1289	327	[a]
cis-$[Ru(bpy)_2(CO)(OCHO)]^+PF_6^-$[b] (**4a**)	spectroscopy	η^1	1621	1282	339	[a]
cis-$[Ru(bpy)_2(CO)(OCHO)]^+PO_2F_2$ (**4b**)	X-ray	η^1	1621	1282	339	[a]
trans-Ru(dmpe)(OCHO)(H)[c]	X-ray	η^1	1603	1329	274	[44]
$(PPh_3)_2Cu(OCHO)$	X-ray	η^2	1585	1350	235	[10,45]
cis, trans-$Re(CO)_2(PPh_3)_2(OCHO)$ (**6**)	spectroscopy	η^2	1547	1358	189	[a]
mer-$Ru(H)(PPh_3)_3(OCHO)$	X-ray	η^2	1553	1310	243	[46,47]
trans-$Ru(CO)(PPh_3)_2(HC{=}CHPh)(OCHO)$	X-ray	η^2	1555	1358	197	[5]
$Mo(H)(PMe_3)_4(OCHO)$ (trans H and formate)	X-ray	η^2	1570	1360	210	[48]
$[CpTi(OCHO)]_2(C_{10}H_8)$	X-ray	μ_2–η^1	1664	1205	459	[49]
$[Pd(PPh_3)(Me)(OCHO)]_2$	X-ray	μ_2–η^2	1595	1349	246	[50]
$[Rh(cod)(OCHO)]_2$[d]	X-ray	μ_2–η^2	1590	1354	236	[51]
$[Rh(cod)(OCHO)Rh(CO)_2$[d]	spectroscopy	μ_2–η^2	1590	1358	232	[51]
$[Rh(CO)_2(OCHO)]_2$	spectroscopy	μ_2–η^2	1570	1345	225	[51]
$[CpRe(NO)(CO)]_2(OCHO)$	spectroscopy	μ_2–η^2	1560	1315	245	[52]
cis, cis–$[Re(CO)_4(PPh_3)]_2(OCHO)^+PF_6^-$ (**7**)	spectroscopy	μ_2–η^2	1563	1395	168	[a]

[a] IR data from this work.
[b] bpy=2, 2′-bipyridine.
[c] dmpe=bis(1,2-dimethylphosphino)ethane.
[d] cod=1, 5-cyclooctadiene.

with organic acetates [11–13], the band at 1380 cm^{-1} is assigned to the symmetric scissoring vibration of the acetate methyl group; the other two bands are assigned to ν_{asym} and ν_{sym} of the carboxylate ligand, respectively. This particular problem may not be resolved readily by preparing the isotopically substituted compound since all three bands will sometimes move [11–13].

All of the compounds in Fig. 6 have triphenylphosphine ligands which show a pair of bands in this region, typically at 1430 and 1480 cm^{-1}, in addition to those of the carboxylates. For the η^2-coordinated acetate complexes, only the manganese complex **11** clearly shows all of the expected bands; in the other acetate complexes, there is overlapping of one of the bands of the phosphine ligand with one of the ν_{OCO} bands of the acetate ligand. As is the case with η^2-coordinated formate complexes (spectra of compound **6** shown in Fig. 6 for comparison), the carboxylate ν_{asym} band in the acetates moves to lower frequency; however, *both* of the other acetate bands in the compound move to higher frequency. The bands for the acetate ligand, in this region, in **11** are assigned as follows: ν_{asym} at 1521 cm^{-1}, ν_{sym} at 1425 cm^{-1} and δ_{C-H} at 1460 cm^{-1}. For comparison, the structurally characterized benzoate complex, *mer*-$Ir[P(CH_3)_3](H)(\eta^2\text{-}O_2CPh)$, shows the carboxylate bands at 1510 and 1428 cm^{-1} [35]. Note that the intensities of the bands assigned to the carboxylate in **11** are very low as are the ones in the η^2-type formate **6** shown in Fig. 6 (compare the intensities of the carboxylate bands against those for the phosphine ligands, in the 1430 and 1480 cm^{-1} region, in these two compounds and the same bands in any of the complexes illustrated in Fig. 4). The reduction in intensities of the carboxylate bands is a characteristic of η^2-type formates and acetates as compared to their η^1-type counterparts. The bands due to the triphenylphosphine ligands in **11** are thus identified as the ones at 1471 cm^{-1} and 1435 cm^{-1}, band positions which are typical of these ligands in this region. The $\Delta\nu$ for the η^2-type acetate complex, **11,** is 106 cm^{-1} and is much smaller than the value for monodentate acetate complexes (as is observed in comparisons of these two types of formates).

Summary data for the ν_{OCO} bands for three bonding types of acetate complexes are listed in Table 5. For the η^1-type complexes, the ν_{asym} band position is similar to that for the related formate complexes; a range of 1612 to 1646 cm^{-1} is observed. However, the ν_{sym} band is at higher frequency (1300–1323 cm^{-1}) than in the formate complexes giving a median value for $\Delta\nu$ of 316 cm^{-1}. For the η^2-type acetates (Table 5) the ν_{asym} bands vary from 1515 to 1562 cm^{-1} and the ν_{sym} band position varies from 1411 to 1425 cm^{-1}. However, there are some structural differences among the example compounds; X-ray data have been obtained recently for $In(tpp)(OCOCH_3)$ (tpp= *meso*-tetraphenylporphyrin) which show differences in the

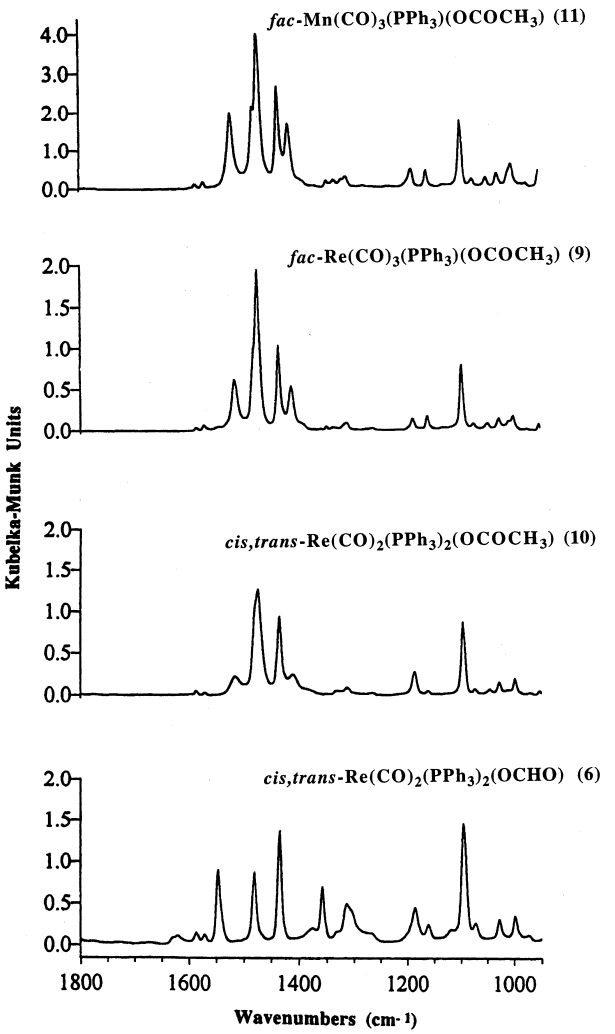

Fig. 6. DRIFTS spectra (1800–950 cm^{-1}) for complexes **6**, **9**, **10**, and **11**.

In–O bond lengths: 2.322(4) and 2.215(4) Å [36]. The investigators described the bonding as ''asymmetric bidentate'' and noted that $\Delta\nu$ for the compound is significantly larger (141 cm^{-1}) than is typical for complexes with symmetrically-bound η^2-type acetate groups.

As with formate complexes, compounds having μ_2–η^2-bound acetate ligands can exist in several different geometric forms. The compounds listed in Table 5 are ones that are structurally constrained to be of the syn, syn type. Both carboxyl C–O stretching bands are moved to higher frequencies in comparison to the η^2-bound types; the $\Delta\nu$ for the examples shown has an average value of 111 cm^{-1}. This value is very similar to the median of 104 cm^{-1} for the symmetrically bonded η^2 complexes of this type (first three entries of the η^2 type in Table 5).

Fig. 5 shows DRIFTS spectra of η^1-type formate, acetate and trifluoroacetate complexes derived from the *cis*-$Ru(bpy)_2(CO)^+$ fragment. All of the compounds show three weak bands in the 1450 cm^{-1} region which are due to the bipyridine ligands; they differ slightly in intensity from one compound to another. The widest separation of the carboxylate ν_{OCO} bands is in the formate complex, (339 cm^{-1}); the trifluoroacetate shows $\Delta\nu$=298 cm^{-1} and the acetate shows a separation of 304 cm^{-1} for these bands. Also, the acetate methyl C–H bending vibration is readily seen at 1360 cm^{-1}. Particularly noteworthy is the vastly reduced intensity of the ν_{sym} band (1403 cm^{-1}) in the trifluoroacetate complex relative to the ν_{asym} band; this appears to be a characteristic of the η^1-type of trifluoroacetate complex. Strong bands in the 1200 cm^{-1} region are assigned to vibrations of the CF_3 group [11–13,37–40].

Examples of complexes demonstrating just two bonding types for the trifluoroacetate ligand are available and are shown in Table 5. Because the electron-withdrawing characteristics of the CF_3 group reduces the nucleophilicity of the carbonyl oxygen in the η^1 complexes, ligand displacement reactions which are used to prepare η^2-type formates and acetates will not proceed with trifluoroacetates. Only the η^1 and μ_2–η^2-types are available for comparison. The electron-withdrawing characteristics of the trifluoromethyl group are also responsible for moving the ν_{asym} band in both classes of compounds to higher frequency values (1685–1713 cm^{-1} in the η^1-type and at 1682 cm^{-1} in the one example bridging type); the band in the η^1 trifluoroacetate complexes is highest for this type, but does not change very much for the bridging complexes. The $\Delta\nu$ for the η^1 type of trifluoroacetate is relatively large at a median value of 293 cm^{-1} and much less, 228 cm^{-1}, for the bridging type.

2. Conclusions

Spectral data for four distinct classes of formate complexes and three classes of acetates are now available, but the low donor characteristics of the trifluoroacetoxy oxygen atoms make the CF_3CO_2 group a much less versatile ligand and limits its complexes to those in which this ligand is monodentate at each metal center. In addition to the bonding type, the nature of the R group in the carboxylate ligand, OC(O)R, has a large impact on the IR band positions for ν_{OCO} in all classes of compounds. The electron-withdrawing CF_3 group has the greatest impact, moving both carboxylate bands to higher frequencies than those in the corresponding formate and acetate complexes. For formate and acetate complexes, the intensities of both ν_{OCO} bands in compounds with η^2-coordinated ligands are much reduced as compared to their η^1-bound analogs. For example, compare the spectra for formate **5** (η^1) in Fig. 4 to that for formate **6** (η^2) in Fig. 6; both compounds have two triphenylphosphine ligands.

The $\Delta\nu$ values, within each ligand type, vary regularly with the nature of bonding to the metal centers. Compounds with chelated carboxyl oxygens have much smaller $\Delta\nu$ values than their monodentate counterparts, although the type of chelation (η^2 or μ_2–η^2) doesn't appear to have further impact. Additionally, with the complexes having

Table 5
Carboxylate stretching frequencies of acetate and trifluoroacetate complexes

Compound	Structure assignment	Bonding	ν_{asym} (CO_2)	ν_{sym} (CO_2)	$\Delta\nu$	Ref
$Cp_2Ti(CH_3)(OCOCH_3)$	spectroscopy	η^1	1646	1300	346	[53]
mer, trans-$Re(CO)_3(PPh_3)_2(OCOCH_3)$	spectroscopy	η^1	1612	1323	289	[a], [17]
cis-$[Ru(bpy)_2(CO)(OCOCH_3)]^+PF_6^-$ (**8**)	spectroscopy	η^1	1621	1317	304	[a]
$Pt(dppf)(OCOCH_3)_2$c	X-ray	η^1	1625 (1595)	1308	317 (287)	[54]
fac-$Re(CO)_3(PPh_3)(OCOCH_3)$ (**9**)	X-ray	η^2	1515	1412	103	[a]
cis, trans-$Re(CO)_2(PPh_3)_2(OCOCH_3)$ (**10**)	X-ray	η^2	1516	1411	105	[a, 17]
fac-$Mn(CO)_3(PPh_3)(OCOCH_3)$ (**11**)	spectroscopy	η^2	1521	1425	106	[a]
$In(tpp)(OCOCH_3)$	X-ray	η^2	1562	1421	141	[36]
$[Rh(CO)(PCy_3)]_2(OCOCH_3)(\mu\text{-}\sigma, \sigma\text{-}C{=}C{=}CPh_2)$	X-ray	$\mu_2\text{-}\eta^2$	1538	1440	98	[55]
$[Rh(CO)(PCy_3)]_2(OCOCH_3)(\mu\text{-}\eta^1{:}\eta^2\text{-}C_2Ph)$	X-ray	$\mu_2\eta^2$	1575	1450	125	[56]
$Cp_2Ti(CH_3)(OCOCF_3)$ (**12**)	spectroscopy	η^1	1701	1422	279	[a]
cis-$Re(CO)_4(PPh_3)(OCOCF_3)$ (**13**)	spectroscopy	η^1	1698	1411	287	[a]
mer, trans-$Re(CO)_3(PPh_3)_2(OCOCF_3)$ (**14**)	spectroscopy	η^1	1685	1412	273	[a]
cis-$[Ru(bpy)_2(CO)(OCOCF_3)]^+PF_6^-$ (**15**)	spectroscopy	η^1	1701	1403	298	[a]
$Pt(dppm)(OCOCF_3)_2$[b]	X-ray	η^1	1713 (1698)	1406	307 (292)	[54]
$Re_2(NBu^t)_4(\mu\text{-}O)(\mu\text{-}OSiMe_3)_3(OCOCF_3)$	X-ray	$\mu_2-\eta^2$	1682	1454	228	[57]

[a] IR data from this work.
[b] dppm=bis(diphenylphosphino)methane.
[c] dppf=1, 1′-bis(diphenylphosphino)ferrocene.

chelated carboxyl ligands, the ν_{OCO} bands shift their positions greatly, with the ν_{asym} band moving to lower frequency and the ν_{sym} band moving to higher frequency, as compared to the monodentate complexes.

3. Experimental

3.1. General procedures.

All reactions were carried out under a nitrogen atmosphere either in Schlenkware or in a Vacuum Atmospheres glovebox. The solvents used in the glovebox were distilled under N_2 from the following drying agents: CH_2Cl_2 with P_2O_5 hexanes and toluene with Na/benzophenone. Reagent grade acetonitrile, ethanol, and diethyl ether were used as received without further purification. Formic acid (95%, aqueous), acetic acid, and trifluoroacetic acid were purchased from Aldrich Chemical Co. and used as received. *cis*-$Re(CO)_4(PPh_3)(CH_3)$ [58], *cis*-$Re(CO)_4(PPh_3)(FBF_3)$ [20], *mer, trans*-$Re(CO)_3(PPh_3)_2H$ [21], *mer, trans*-$Re(CO)_3(PPh_3)_2(\eta^1\text{-}OCOCH_3)$ [17], *cis*-$[Ru(bpy)_2(CO)H]PF_6$ [59], and $Cp_2Ti(CH_3)(\eta^1\text{-}OCOCH_3)$ [53] were prepared according to literature methods. The ^1H, ^{13}C, and ^{31}P NMR spectra were recorded on a Bruker AMX-500 spectrometer; the ^1H and ^{13}C chemical shifts were referenced to residual protons and carbons in the deuterated solvents, respectively. The ^{31}P chemical shifts were determined using H_3PO_4(85%) as the external standard. Infrared spectra were obtained by the DRIFTS technique (diffuse reflectance infrared Fourier transform spectroscopy [60]) and were recorded on an ATI Mattson RS-1 FTIR Spectrometer using a Minidiff DRIFTS accessory (Graseby Specac. Inc.). Melting points were determined on a Thomas-Hoover capillary melting point apparatus and are uncorrected. Elemental analyses were performed by Midwest Microlab, Indianapolis, IN.

3.2. Synthesis of cis-$Re(CO)_4(PPh_3)(\eta^1\text{-}OCHO)$ (1)

Cis-$Re(CO)_4(PPh_3)(CH_3)$ (0.20 g, 0.35 mmol) was placed in a flask, followed by excess formic acid (5 ml). The mixture was heated to 50°C with stirring for 2 h, then cooled to room temperature and evaporated to dryness. The residue was triturated with hexane, then the hexane extracts were evaporated under vacuum to leave a white solid (quantitative yield), mp 109°C.

Anal. calcd for $C_{23}H_{16}O_6PRe$: C, 45.62; H, 2.66. Found: C, 45.54; H, 2.70. IR (DRIFTS, KCl): ν_{CO} 2101, 2018, 1983, and 1960 cm^{-1}; ν_{OCO} 1626 and 1277 cm^{-1}. ^1H NMR ($CDCl_3$): δ 7.64 (s, OCHO); 7.45 (m, Ph). ^{13}C NMR ($CDCl_3$): δ 187.45 (s, CO); 187.38 (s, CO); 184.32 (d, J_{CP}=53.7 Hz, CO); 168.22 (d, J_{CP}=1.2 Hz, OCHO); 133.39 (d, J_{CP}=11.7 Hz, Ph); 131.28 (d, J_{CP}=47.8 Hz, Ph); 131.14 (d, J_{CP}=1.2 Hz, Ph); 128.86 (d, J_{CP}=10.1 Hz, Ph). ^{31}P NMR ($CDCl_3$): δ 12.11.

3.3. Synthesis of $Cp_2Ti(CH_3)(\eta^1\text{-}OCHO)$ (2)

$Cp_2Ti(CH_3)_2$ [61], 0.52 g (2.50 mmol), was dissolved in CH_2Cl_2 (20 ml), formic acid (0.10 ml, 95%, 2.5 mmol) was added and the mixture was stirred for 30 min. The mixture was evaporated to dryness under vacuum and the

residue was recrystallized from CH_2Cl_2/hexanes to yield a red solid, 0.55 g (92%), mp 117–118°C (dec).

Anal. calcd for $C_{12}H_{14}O_2Ti$: C, 60.53; H, 5.93. Found: C, 60.72; H, 6.20. IR (DRIFTS, KCl): ν_{OCO} 1652, 1636, 1270, and 1258 cm^{-1}. ^1H NMR (CD_2Cl_2): δ 8.07 (s, 1, OCHO); 6.19 (s, 10, Cp); 0.70 (s, 3, CH_3). ^{13}C NMR (CD_2Cl_2): δ 166.23 (OCHO); 115.07 (Cp); 45.99 (CH_3).

3.4. Characterization data for $Cp_2Ti(\eta^1\text{-}OCHO)_2$ (3) [16]

Anal. calcd for $C_{12}H_{12}O_4Ti$: C, 53.76; H, 4.51. Found: C, 53.68; H, 4.47. IR (DRIFTS, KCl): ν_{OCO} 1644, 1290, and 1273 cm^{-1}. ^1H NMR (CD_2Cl_2): δ 8.46 (s, 2, OCHO); 6.55 (s, 10, Cp). ^{13}C NMR (CD_2Cl_2): δ 167.05 (OCHO); 119.10 (Cp).

3.5. Synthesis of cis-$[Ru(bpy)_2(CO)(\eta^1\text{-}OCHO)]PF_6$ (4a)

Cis-$[Ru(bpy)_2(CO)(H)]PF_6$ (0.100 g, 0.17 mmol) was placed in a flask, formic acid (5 ml) was added and the mixture was stirred for 1 hr. The mixture was evaporated to dryness under vacuum, then dissolved in CH_3CN (10 ml) and treated with excess NH_4PF_6 (aq, 10 ml) to afford anion-exchange. The resulting solution was concentrated to half of its original volume and a yellow solid which precipitated was collected by filtration and dried under vacuum, 0.095 g (88%), mp>250°C.

IR (DRIFTS, KCl): ν_{CO} 1972 cm^{-1}; ν_{OCO} 1621 and 1281 cm^{-1} (lit. [16] (CH_2Cl_2): ν_{CO} 1984 cm^{-1}). ^1H NMR (CD_3CN): δ 9.54 (d, J=5.7 Hz, bpy); 8.85 (d, J=5.7 Hz, bpy); 7.83 (s, OCHO); 8.52–7.27 (m, bpy). ^{13}C NMR (CD_3CN): δ 201.67 (CO); 169.04 (OCHO); 158.05–124.54 (20 resonances, bpy).

3.6. Synthesis of cis-$[Ru(bpy)_2(CO)(\eta^1\text{-}OCHO)]PF_2O_2$ (4b)

Cis-$[Ru(bpy)_2(CO)(H)]PF_6$ (0.12 g, 0.20 mmol) was placed in a flask, formic acid (5 ml) was added. The mixture was heated to reflux for 1 hr, then formic acid was removed under vacuum. The residue was extracted with CH_3CN (20 ml) and the extract filtered. Ether (60 ml) was added to precipitate a yellow solid; the solid was re-crystallized from CH_3CN/ether to yield yellow crystals, 0.043 g (36%).

Anal. calcd for $C_{22}H_{17}F_2N_4O_5PRu$: C, 44.98; H, 2.92. Found: C, 45.39; H, 3.06. The ^1H and ^{13}C NMR spectral properties are identical to those of *cis*-$[Ru(bpy)_2(CO)(\eta^1\text{-}OCHO)]PF_6$ (**4a**). ^{31}P NMR (CD_3CN): δ −12.93 (t, J_{PF}= 948.0 Hz).

3.7. Synthesis of mer, trans-$Re(CO)_3(PPh_3)_2(\eta^1\text{-}OCHO)$ (5)

Mer, *trans*-$Re(CO)_3(PPh_3)_2(H)$ (0.10 g, 0.13 mmol) was placed in a flask. Formic acid (10 ml) was added. The mixture was heated at reflux for 30 min. The solvent was removed under vacuum to yield a white solid, 0.105 g (quantitative yield).

IR (DRIFTS, KCl): ν_{CO} 2045, 1943, and 1902 cm^{-1}; ν_{OCO} 1616 and 1289 cm^{-1} (lit. [17]: ν_{CO} 2040, 1950, and 1900 cm^{-1}; ν_{OCO} 1620 and 1300 cm^{-1}). ^1H NMR ($CDCl_3$): δ 7.54–7.34 (m, Ph); 7.07 (s, OCHO). ^{13}C NMR ($CDCl_3$): δ6 195.08 (t, J_{CP}=6.1 Hz, CO); 194.41 ((t, J_{CP}=9.2 Hz, CO); 167.89 (s, OCHO); 133.70 (t, J_{CP}=5.6 Hz, Ph); 133.28 (t, J_{CP}=23.9 Hz, Ph); 130.22 (s, Ph); 128.25 (t, J_{CP}=5.1 Hz, Ph). ^{31}P NMR ($CDCl_3$): δ 18.38.

3.8. Synthesis of cis, trans-$Re(CO)_2(PPh_3)_2(\eta^2\text{-}OCHO)$ (6)

Mer, trans-$Re(CO)_3(PPh_3)_2(\eta^1\text{-}OCHO)$ (0.05 g, 0.06 mmol) was dissolved in toluene (10 ml) and the solution was heated at reflux for 1 h. After cooling to room temperature, the solvent was removed under vacuum leaving a white residue which was washed with ethanol (4×5 ml) then dried under vacuum, 0.04 g (81%).

IR (DRIFTS, KCl): ν_{CO} 1925 and 1849 cm^{-1}; ν_{OCO} 1547 and 1358 cm^{-1} (lit. [17]: ν_{CO}, 1930 and 1850 cm^{-1}; ν_{OCO}, 1550 and 1360 cm^{-1}). ^1H NMR ($CDCl_3$): δ 7.83 (t, J_{HP}=3.6 Hz, OCHO); 7.44–7.37 (m, Ph). ^{13}C NMR ($CDCl_3$): δ 201.46 (t, J_{CP}=7.1 Hz, CO); 173.86 (t, J_{CP}= 2.0 Hz, OCHO); 134.17 (t, J_{CP}=6.1 Hz, Ph); 132.47 (t, J_{CP}=22.9 Hz, Ph); 130.05 (s, Ph); 128.28 (t, J_{CP}=5.1 Hz, Ph). ^{31}P NMR ($CDCl_3$): δ 33.65.

3.9. Synthesis of cis, cis-$([Re(CO)_4(PPh_3)]_2(\mu_2\text{–}\eta^2\text{-}OCHO)]BF_4$ (7)

Cis-$Re(CO)_4(PPh_3)(\eta^1\text{-}OCHO)$ (**1**; 0.07 g, 0.12 mmol) and *cis*-$Re(CO)_4(PPh_3)(FBF_3)$ (0.08 g, 0.12 mmol) were combined in a flask. CH_2Cl_2 (10 ml) was added. The mixture was stirred for 1 h and then solvent was removed under vacuum to afford a white solid, 0.150 g (quantitative yield), mp 114°C.

Anal. calcd for $C_{45}H_{31}BF_4O_{10}P_2Re_2$: C, 43.14; H, 2.49. Found: C, 42.83; H, 2.62. IR (DRIFTS, KCl): ν_{CO} 2114, 2012, and 1955 cm^{-1} ν_{OCO} 1562 and 1359 cm^{-1}. ^1H NMR (CD_2Cl_2): δ, 7.58–7.38 (m, Ph); 6.94 (s, OCHO);. ^{13}C NMR (CD_2Cl_2): δ 186.90 (d, J_{CP}=8.8 Hz, CO); 185.64 (d, J_{CP}=6.3 Hz, CO); 183.73 (d, J_{CP}=52.5 Hz, CO); 177.84 (s, OCHO); *135.55* (d, J_{CP}=10.1 Hz, Ph); 132.40 (d, J_{CP}=1.2 Hz, Ph); 129.85 (d, J_{CP}=49.0 Hz, Ph); 129.45 (d, J_{CP}=10.1 Hz, Ph). ^{31}P NMR (CD_2Cl_2): δ 13.31.

3.10. Synthesis of cis-$[Ru(bpy)_2(CO)(\eta^1\text{-}OCOCH_3)]PF_6$ (8)

Cis-$[Ru(bpy)_2(CO)(H)]PF_6$ (0.05 g, 0.08 mmol) was placed in a flask together with acetic acid (5 ml). The mixture was heated at 60°C for 2.5 h, then acetic acid was

removed under vacuum. The residue was dissolved in CH_3CN (10 ml) and treated with NH_4PF_6 (aq, 10 ml) to afford anion-exchange. The resulting solution was concentrated to half of its original volume, resulting in precipitation of a yellow solid which was collected by filtration and dried under vacuum, 0.04 g (76%), mp>250°C.

Anal. calcd for $C_{23}H_{19}F_6N_4O_3PRu$: C, 42.80; H, 2.97. Found: C, 42.50; H, 3.04. IR (DRIFTS, KCl): ν_{CO} 1964 cm^{-1} ν_{OCO} 1621 and 1317 cm^{-1}. ^1H NMR (CD_3CN): δ 9.55 (d, J=5.7 Hz, bpy); 8.88 (d, J=5.7 Hz, bpy); 8.49–7.25 (m, bpy) 1.70 (s, CH_3). ^{13}C NMR (CD_3CN): δ 201.95 (CO); 177.78 (OCO); 158.21–124.44 (20 resonances, bpy); 23.21 (CH_3).

3.11. Synthesis of fac-Re(CO)$_3$(PPh$_3$)(η^2-OCOCH$_3$) (**9**)

Cis-$Re(CO)_4(PPh_3)(CH_3)$ (0.103 g, 0.18 mmol) was placed in a flask together with acetic acid (5 ml). The mixture was stirred at 60°C for 6 h, then acetic acid was removed under vacuum. The residue was recrystallized from CH_2Cl_2/hexane to yield colorless crystals, 0.079 g (73%), mp 195–196°C.

Anal. calcd for $C_{23}H_{18}O_5PRe$: C, 46.70; H, 3.07. Found: C, 46.60; H, 3.14. IR (DRIFTS, KCl): ν_{CO} 2030, 1937, and 1901 cm^{-1} ν_{OCO} 1515 and 1412 cm^{-1}. ^1H NMR ($CDCl_3$): δ, 7.50–7.33 (m, Ph); 1.10 (s, CH_3). ^{13}C NMR ($CDCl_3$): δ 195.18 (d, J_{CP}=7.1 Hz, CO); 190.47 ((d, J_{CP}=72.7 Hz, CO); 189.18 (d, J_{CP}=2.5 Hz, OCO); 134.24 (d, J_{CP}=11.2 Hz, Ph); 130.91 (d, J_{CP}=2.0 Hz, Ph); 129.33 (d, J_{CP}=45.3 Hz, Ph); 128.74 (d, J_{CP}=9.7 Hz, Ph); 24.09 (s, CH_3). ^{31}P NMR ($CDCl_3$): δ 29.33.

3.12. Synthesis of cis, trans-Re(Co)$_2$(PPh$_3$)$_2$(η^2-OCOCH$_3$) (**10**)

This compound was prepared by a modification of the previous method [16]. *Mer, trans*-$Re(CO)_3(PPh_3)_2(H)$ (0.10 g, 0.13 mmol) was placed in a flask together with acetic acid (10 ml). The mixture was heated to 85°C for 5 h, then acetic acid was removed under vacuum. The white residue was washed with ethanol (4×5 ml) and dried under vacuum, 0.08 g (91%).

IR (DRIFTS, KCl): ν_{CO} 1925 and 1851 cm^{-1}; ν_{OCO} 1516 and 1411 cm^{-1} (lit. [17]: ν_{CO} 1930 and 1850 cm^{-1} ν_{OCO}, 1515 cm^{-1}). ^1H NMR ($CDCl_3$): δ 7.43–7.38 (m, Ph); 0.42 (s, CH_3). ^{13}C NMR ($CDCl_3$): δ 201.88 (t, J_{CP}=7.1 Hz, CO); 185.59 (t, J_{CP}=4.0 Hz, OCO); 134.24 (t, J_{CP}=5.6 Hz, Ph); 132.56 (t, J_{CP}=22.4 Hz, Ph); 129.87 (s, Ph); 128.20 (t, J_{CP}=4.6 Hz, Ph); 23.49 (s, CH_3). ^{31}P NMR ($CDCl_3$): δ 33.14.

3.13. Spectral properties of fac-Mn(CO)$_3$(PPh$_3$)(η^2-OCOCH$_3$) (**11**)

A sample of this compound was available from previous work [22]. It showed IR(DRIFTS, KCl) ν_{CO} 2030, 1949, 1913 cm^{-1}; ν_{OCO} 1521 and 1415 cm^{-1}. ^1H NMR ($CDCl_3$): δ 7.41 (m, 15H, Ph); 1.02 (s, 3H, CH_3). ^{13}C NMR ($CDCl_3$) δ 222.63 (CO); 212.67 (CO); 185.84 (OCO); 134.27 (d, J_{PC}=8.1 Hz, Ph); 136.63 (s, Ph); 130.17 (d, J_{PC}=38.1 Hz, Ph); 128.56 (d, J_{PC}=6.1 Hz, Ph), 22.92 (s, CH_3).

3.14. Synthesis of Cp$_2$Ti(CH$_3$)(η^1-OCOCF$_3$) (**12**)

$Cp_2Ti(CH_3)_2$ (1.60 g, 7.69 mmol) was dissolved in CH_2Cl_2 (20 ml) and cooled to 0°C. Trifluoroacetic acid (0.60 ml, 99%, 7.7 mmol) was added dropwise. The mixture was stirred for 30 min. The solvent was removed under vacuum. The residue was recrystallized from toluene/hexanes to yield a red solid, 2.12 g (90%), mp 117–118°C (dec).

Anal. calcd for $C_{13}H_{13}F_3O_2Ti$: C, 51.00; H, 4.28. Found: C, 51.14; H, 4.38. IR (DRIFTS, KCl): ν_{OCO} 1700 and 1240 cm^{-1}. ^1H NMR (C_6D_6): δ 5.62 (s, 10, Cp); 0.97 (s, 3, CH_3). ^{13}C NMR (C_6D_6): δ 160.06 (q, J_{CF}=39.1 Hz, OCO); 115.41 (Cp); 51.06 (CH_3).

3.15. Synthesis of cis-Re(CO)$_4$(PPh$_3$)(η^1-OCOCF$_3$) (**13**)

Cis-$Re(CO)_4(PPh_3)(CH_3)$ (0.20 g, 0.35 mmol) was dissolved in CH_2Cl_2 (10 ml) and trifluoroacetic acid (0.030 ml) was added. The mixture was stirred for 30 min. Then the mixture was evaporated to dryness under vacuum. The gummy residue was treated with hexane. The hexane was removed under vacuum to leave a white solid, 0.23 g (quantitative yield), mp 92°C.

Anal. calcd for $C_{24}H_{15}F_3O_6PRe$: C, 42.79; H, 2.24. Found: C, 42.70; H, 2.25. IR (DRIFTS, KCl): ν_{CO} 2105, 2003, and 1958 cm^{-1}; ν_{OCO} 1698 and 1410 cm^{-1}. ^1H NMR ($CDCl_3$): δ, 7.50–7.45 (m, Ph). ^{13}C NMR ($CDCl_3$): δ, 186.94 (d, J_{CP}=5.6 Hz, CO); 186.83 (d, J_{CP}=9.2 Hz, CO); 183.86 (d, J_{CP}=56.0 Hz, CO); 162.25 (d of q, J_{CP}=2.0 Hz, J_{CF}=37.6 Hz, OCO); 133.23 (d, J_{CP}=11.2 Hz, Ph); 131.34 (d, J_{CP}=2.5 Hz, Ph); 130.73 (d, J_{CP}=48.8 Hz, Ph); 129.02 (d, J_{CP}=10.2 Hz, Ph); 114.23 (q, J_{CF}=289.4 Hz, CF_3). ^{31}P NMR ($CDCl_3$): δ 11.88.

3.16. Synthesis of mer, trans-Re(CO)$_3$(PPh$_3$)$_2$(η^1-OCOCF$_3$) (**14**)

This compound was prepared by a modification of the literature method [23]. *Mer, trans*-$Re(CO)_3(PPh_3)_2(H)$ [21] (0.20 g, 0.25 mmol) was dissolved in CH_2Cl_2 (20 ml). The solution was then heated to reflux and CF_3COOH (1 ml) was added. The mixture was kept at reflux for 30 min then evaporated to dryness under vacuum. The residue was washed with ethanol (4×15 ml) and dried under vacuum (0.20 g (90%).

IR (DRIFTS, KCl): ν_{CO} 2053, 1952, and 1901 cm^{-1}

ν_{OCO} 1685 and 1412 cm^{-1} (lit. [17]: ν_{CO} 2040, 1950, and 1895 cm^{-1}; ν_{OCO} 1680 and 1410 cm^{-1}). ^{1}H NMR (CD_2Cl_2): δ 7.59–7.36 (m, Ph). ^{13}C NMR (CD_2Cl_2): δ 194.85 (t, J_{CP}=5.6 Hz, CO); 194.37 (t, J_{CP}=8.8 Hz, CO); 162.60 (q, J_{CF}=36.3 Hz OCO); 133.84 (t, J_{CP}=5.6 Hz, Ph); 133.16 (t, J_{CP}=24.1 Hz, Ph); 130.94 (s, Ph); 128.92 (t, J_{CP}=5.0 Hz, Ph); 114.32 (q, J_{CF}=283.8 Hz, CF_3). ^{31}P NMR (CD_2Cl_2): δ 17.67.

3.17. Synthesis of cis-[Ru(bpy)$_2$(CO)(η^1-OCOCF$_3$)]PF$_6$ (**15**)

Cis-[Ru(bpy)$_2$(CO)(H)]PF_6 (0.05 g, 0.08 mmol) was dissolved in CH_2Cl_2 (10 ml) then trifluoroacetic acid (1 ml) was added. The mixture was stirred for 20 min then evaporated to dryness under vacuum. The residue was dissolved in CH_2Cl_2 (5 ml); diethyl ether (20 ml) was then added to precipitate a yellow solid. The solid was collected by filtration and dissolved in CH_3CN (10 ml) and treated with NH_4PF_6 (aq, 10 ml) to afford anion-exchange. The resulting solution was concentrated to half of its original volume and the yellow solid which precipitated was collected by filtration and dried under vacuum, 0.04 g (60%), mp>250°C.

Anal. calcd for $C_{23}H_{,6}F_9N_4O_3PRu$: C, 39.49; H, 2.31. Found: C, 39.58; H, 2.55. IR (DRIFTS, KCl): ν_{CO} 1990 cm^{-1}; ν_{OCO} 1701 and 1403 cm^{-1}. ^{1}H NMR (CD_3CN): δ 9.55 (d, J=5.7 Hz, bpy); 8.76 (d, J=5.7 Hz, bpy); 8.56–7.28 (m, bpy). ^{13}C NMR (CD_3CN): δ 200.48 (CO); 163.66 (q, J_{CF}=35.6 Hz, OCO); 158.22–124.68 (20 resonances, bpy); 114.70 (q, J_{CF}=289.9 Hz, CF_3).

3.18. X-ray crystal structure of [cis-Ru(bpy)$_2$(CO)(OCHO)]PF$_2$O$_2$ (**4b**)

A yellow crystal of [*cis*-Ru(bpy)$_2$(CO)(OCHO)]PF_20_2, grown by diffusing diethyl ether over a CH_3CN solution, was mounted on a glass fiber with epoxy cement. Data were collected on an Enraf-Nonius CAD-4 diffractometor at room temperature. Crystal data, data collection, and refinement parameters are summarized in Table 1. The structure was solved by direct methods and completed by a series of least-squares and difference Fourier synthesis. An empirical correction for absorption (Ψ scans) was applied. All non-hydrogen atoms were refined with anisotropic thermal parameters except for the partial occupancy F and O atoms of the disordered $PF_2O_2^-$ anion. The disorder consists of a P atom with four sets of F_2O_2 atoms, each at 25% occupancy. These atoms were refined with isotropic thermal parameters. The hydrogen atoms were located by difference maps and included as fixed isotropic contributions (B=1.2 B of attached atom). Full-matrix least-squares refinements were carried out for 3266 reflections with ($I>3\sigma(I)$). A final R index of 0.055 was obtained for 344 variables. All calculations were performed using the teXsan package (Molecular Structure Corporation) [62].

3.19. X-ray crystal structure of fac-Re(CO)$_3$(PPh$_3$)(η^2-OCOCH$_3$) (**9**)

A colorless crystal of *fac*-Re(CO)$_3$(PPh_3)(η^2-$OCOCH_3$), grown from CH_2Cl_2/hexanes at −30°C, was mounted on a glass fiber with epoxy cement. Data were collected on an Enraf-Nonius CAD-4 diffractometor equipped with a graphite monochromator. Crystal data, data collection, and refinement parameters are listed in Table 1. Of 5312 unique reflections, 3808 were considered observed ($I>3\sigma$(I)). The structure was solved by direct methods. An empirical correction for absorption (Ψ scans) was applied. All non-hydrogen atoms were refined with anisotropic thermal parameters. The hydrogen atoms were located by difference maps and included as fixed contributions (B=1.2 B of attached atom). A final R index of 0.022 was obtained for 272 variables. All calculations were performed using the teXsan package (Molecular Structure Corporation) [62].

3.20. Supplementary materials

Tables of bond lengths, bond distances, positional and isotropic thermal parameters and general displacement parameters for **4b** and **9** are provided in the Supplementary Materials which have been deposited at the Cambridge Crystallographic Data Base.

Acknowledgements

Support of this work by the National Science Foundation (CHE-9112872) and NSF/KY EPSCoR Program (EHR-9108764) is gratefully acknowledged; also, the X-ray equipment was purchased with assistance from NSF (CHE-9016978). Partial support of the work by the United States Department of Energy, Division of Chemical Sciences (Office of Basic Energy Sciences), Office of Energy Research, is also gratefully acknowledged.

References

[1] P.G. Jessop, T. Ikariya, R. Noyori, Chem. Rev. 95 (1995) 259.
[2] W. Leitner, Angew. Chem. Int. Ed. Engl. 34 (1995) 2207.
[3] D.J. Darensbourg, M.B. Fischer, R.E. Schmidt, B.J. Baldwin, J. Am. Chem. Soc. 103 (1981) 1297.
[4] W. Wills, K.M. Nicholas, Inorg. Chim. Acta 90 (1984) L51.
[5] H. Loumrhari, L. Matas, J. Ros, M.R. Torres, A. Perales, J. Organomet. Chem. 403 (1991) 373.
[6] J.-C. Tsai, K.M. Nicholas, J. Am. Chem. Soc. 114 (1992) 5117.
[7] F.M. Hoffman, M.D. Weisel, Surf. Sci. Lett. (1991) L402.
[8] M.R. Columbia, A.M. Crabtree, P.A. Thiel, Am. Chem. Soc. 114 (1992) 1231.

[9] M.D. Weisel, J.G. Chen, F.M. Hoffmann, Y.-K. Sun, J. Chem. Phys. 97 (1992) 9396.
[10] C. Xu, D.W. Goodman, J. Phys. Chem. 100 (1996) 1753.
[11] O.B. Deacon, R.J. Phillips, Coord. Chem. Rev. 33 (1980) 211.
[12] K. Nakamoto, Infrared and Raman Spectra of Inorganic and Coordination Compounds, 4th ed.; Wiley: New York, 1986.
[13] G. Busca, V. Lorenzelli, Mater. Chem. 7 (1982) 89.
[14] B.P. Sullivan, J.V. Caspar, S.R. Johnson, T.J. Meyer, Organometallics 3 (1984) 1241.
[15] E. Horn, M.R. Snow, Aust. J. Chem. 33 (1980) 2369.
[16] D.H. Gibson, Y. Ding, J.F. Richardson, M.S. Mashuta, Acta. Crystallogr. Sect. C 52 (1996) 1614.
[17] R.F. Bardon, M.Sc. Thesis, University of Louisville, 1994.
[18] G. La Monica, S. Cenini, E. Forni, M. Manassero, V.G. Albano, J. Organomet. Chem. 112 (1976) 297.
[19] T. Wohrle, U. Thewalt, J. Organomet. Chem. 468 (1994) C1.
[20] K. Raab, W. Beck, Chem. Ber. 118 (1985) 3830.
[21] D.H. Gibson, K. Owens, S.K. Mandal, W.E. Sattich, J.O. Franco, Organometallics 8 (1989) 498.
[22] S.K. Mandal, Ph.D. Dissertation, University of Louisville, 1988.
[23] R.F. Bardon, unpublished results.
[24] J.M. Clear, J.M. Kelly, C.M. O'Connell, J.G. Vos, C. J. Cardin, S.R. Costa, A.I. Edwards, J. Chem. Soc. Chem. Commun. (1980) 750.
[25] H. Tanaka, B.-C. Tzeng, H. Nagao, S.-M. Peng, K. Tanaka, Inorg. Chem. 32 (1993) 1508.
[26] H. Nagao, T. Mizukawa, K. Tanaka, Inorg. Chem. 323 (1994) 3415.
[27] K. Toyohara, H. Nagao, T. Adachi, T. Yoshida, K. Tanaka, Chem. Lett. (1996) 27.
[28] D.H. Gibson, J.M. Mebta, M. Ye, J.F. Richardson, M.S. Mashuta, Organometallics 13 (1994) 1070.
[29] J. Ni, Y. Qiu, T.M. Cox, et al., Organometallics 15 (1996) 4669.
[30] R.L. Rardin, W.B. Tolman, S.J. Lippard, New J. Chem. 15 (1991) 417.
[31] W. Tolman, S. Liu, J.G. Bentsen, S.J. Lippard, J. Am. Chem. Soc. 113 (1991) 152.
[32] H.E. Wages, K.L. Taft, S.J. Lippard, Inorg. Chem. 32 (1993) 4985.
[33] M.J. Baldwin, J.W. Kampf, V.J. Peccaro, J. Chem. Soc., Chem. Commun. (1993) 1741.
[34] R. Fornika, E. Dinjus, H. Gorls, W. Leitner, J. Organomet. Chem. 511 (1996) 145.
[35] F.T. Ladipo, J.S. Merola, Inorg. Chem. 32 (1993) 5201.
[36] S.-J. Lin, T.-N. Hong, J.-Y. Tung, J.-H. Chen, Inorg. Chem. 36 (1997) 3886.
[37] R.L. Redington, K.C. Lin, Spectrochem. Acta 27A (1971) 2445.
[38] P.J. Miller, R.A. Butler, E.R. Lippincott, J. Chem. Phys. 57 (1972) 5451.
[39] N.E. Dixon, W.G. Jackson, M.A. Lancaster, G.A. Lawrence, A.M. Sargeson, Inorg. Chem. 20 (1981) 1470.
[40] P.V. Bernhardt, G.A. Lawrence, Polyhedron 6 (1987) 1875.
[41] R.J. McKinney, H.D. Kaesz, J. Am. Chem. Soc. 97 (1975) 3066.
[42] J.M. Kelly, J.G. Vos, Angew. Chem. Int. Ed. Engl. 21 (1982) 628.
[43] R.J. Puddephatt, M.A. Stalteri, Organometallics 2 (1983) 1400.
[44] P.W. Griffiths, J.A. DeHaseth, Fourier Transform Infrared Spectroscopy, Wiley, New York, 1986, Chapter 5.
[45] K. Clauss, H. Bestian, Justus Liebigs Ann. Chem. 654 (1962) 8.
[46] teXsan: Single Crystal Structure Analysis Software, Version 1.6; Molecular Structure Corp.: The Woodlands, TX 77381, 1993.
[47] A. Immirzi, A. Musco, Inorg. Chim. Acta 22 (1977) L35.
[48] J. Hawecker, J.-M. Lehn, R. Ziessel, Helv. Chim. Acta. 69 (1986) 1990.
[49] J. Guilhem, C. Pascard, J.-M. Lehn, R. Ziessel, J. Chem. Soc., Dalton Trans. (1989) 1449.
[50] M.K. Whittlesey, R.N. Perutz, M.H. Moore, Organometallics 15 (1996) 5166.
[51] N. Marsich, A. Camus, G. Nardin, J. Organomet. Chem. 239 (1982) 429.
[52] S. Komiya, A. Yamamoto, J. Organomet. Chem. 46 (1972) C58.
[53] I.S. Kolomnikov, A.I. Gusev, G.G. Aleksandrov, T.S. Lobeeva, Y.T. Struchkov, M.E. Vol'pin, J. Organomet. Chem. 59 (1973) 349.
[54] D. Lyons, G. Wilkinson, M. Thornton-Pett, M.B. Hursthouse, J. Chem. Soc., Dalton Trans. (1984) 695.
[55] J. Ni, Y. Qiu, T.M. Cox, et al., Organometallics 15 (1996) 4669.
[56] V.V. Grushin, C. Bensimon, H. Alper, Organometallics 14 (1995) 3259.
[57] R. Fornikca, E. Dinjus, H. Gorls, W. Leitner, J. Organomet. Chem. 511 (1996) 145.
[58] C.C. Tso, A.R. Cutler, Inorg. Chem. 29 (1990) 471.
[59] A.L. Tan, P.M.N. Low, Z.-Y. Thou, W. Zheng, B.-M. Wu, T.C.W. Mak, T.S.A. Hor, J. Chem. Soc., Dalton Trans. (1996) 2207.
[60] A.J. Edwards, M.A. Esteruelas, F.J. Lahoz, J. Modrego, L.A. Oro, J. Schrickel, Organometallics 15 (1996) 3556.
[61] M.A. Esteruelas, O. Lahuerta, J. Modrego, et al., Organometallics 12 (1993) 266.
[62] V. Saboonchian, A.A. Danopoulos, A. Gutierrez, G. Wilkinson, D.J. Williams, Polyhedron 10 (1991) 2241.